

Intelligent identification for discrete memristive neuron map: An adaptive chaos game optimization algorithm studied from the perspectives of different sample sizes and objective functions

Yuexi Peng(彭越兮), Xinyi Luo(罗馨怡), Zhijun Li(李志军), Mengjiao Wang(王梦蛟), and Minglin Ma(马铭磷)
Citation: Chin. Phys. B, 2026, 35 (**6**): 060507. DOI: 10.1088/1674-1056/ae3690
http://cpb.iphy.ac.cn; http://iopscience.iop.org/cpb

What follows is a list of articles you may be interested in

Color image encryption algorithm using a new four-dimensional hyperchaotic system

Bo Lin(林博), Min Liu(刘敏), and Guodong Ye(叶国栋)
Chin. Phys. B, 2026, 35 (**5**): 050502. DOI: 10.1088/1674-1056/ae0bff

Impact of altruistic preference on the dynamic decision and coordination of joint emission reduction in low-carbon supply chain

Jinchai Lin(林金钗), Chunyan Zheng(郑春艳), Ruguo Fan(范如国), Yuanyuan Wang(王圆缘), Yingqing Zhang(张应青), and Han Song(宋寒)
Chin. Phys. B, 2026, 35 (**4**): 040501. DOI: 10.1088/1674-1056/ae0015

Spiking-bursting alternating chaos mediated by a locally active memristor

Yuxia Li(李玉霞), Xintong Yue(岳新同), Hui Chang(常辉), Baoxing Han(韩宝兴), and Yan Zhang(张燕)
Chin. Phys. B, 2026, 35 (**3**): 030504. DOI: 10.1088/1674-1056/ae44f9

An epidemiological stochastic predator-prey model with prey refuge and harvesting

Israr Ali, Hui Zhang(张慧), Syed Murad Ali Shah, Abdulwasea Alkhazzan, and Yassine Sabbar
Chin. Phys. B, 2026, 35 (**2**): 020503. DOI: 10.1088/1674-1056/adf17f

Energy adaptive regulation of a multifunctional neuron circuit

Xi-Kui Hu(胡锡奎), Juan Yang(杨娟), and Ping Zhou(周平)
Chin. Phys. B, 2026, 35 (**1**): 010503. DOI: 10.1088/1674-1056/ae1451

SPECIAL TOPIC — Biophysical circuits: Modeling & applications in neuroscience

Intelligent identification for discrete memristive neuron map: An adaptive chaos game optimization algorithm studied from the perspectives of different sample sizes and objective functions

Yuexi Peng(彭越兮)[1,†], Xinyi Luo(罗馨怡)[1], Zhijun Li(李志军)[2], Mengjiao Wang(王梦蛟)[2], and Minglin Ma(马铭磷)[2]

[1] *School of Computer Science, Xiangtan University, Xiangtan* 411105, *China*
[2] *School of Automation and Electronic Information, Xiangtan University, Xiangtan* 411105, *China*

(Received 3 November 2025; revised manuscript received 18 December 2025; accepted manuscript online 12 January 2026)

Discrete memristive neuron systems have attracted considerable attention due to their nonlinear dynamical properties, low computational overhead, and ease of hardware implementation. For the practical engineering applications of discrete memristive neuron systems, effective control remains a key issue. Parameter identification using intelligent optimization algorithms is an important approach for controlling complex nonlinear systems. However, classical algorithms are prone to falling into local optima and often exhibit high computational complexity, resulting in slow convergence. Therefore, a new algorithm named adaptive chaos game optimization (ACGO) is proposed to address these issues. By introducing a differential evolution mutation strategy and a Cauchy adaptive parameter mechanism, the ACGO algorithm can effectively balance global exploration and local exploitation capabilities. To verify the effectiveness of the proposed algorithm, it is applied to parameter identification in five discrete memristive neuron maps (DMNMs) and compared with seven intelligent optimization algorithms. Simulation results demonstrate that the ACGO algorithm achieves higher accuracy and faster convergence. In addition, an in-depth investigation is conducted into the effects of sample size and objective function on identification performance. The results indicate that setting the sample size to 4 and selecting the mean squared error (MSE) as the objective function can achieve better identification performance and a high level of robustness.

Keywords: discrete memristive neuron map, parameter identification, chaos game optimization algorithm, sample size

PACS: 05.45.–a

DOI: 10.1088/1674-1056/ae3690 **CSTR:** 32038.14.CPB.ae3690

1. Introduction

Memristors are a new type of electronic device with intrinsic memory characteristics.[1] Since the memristor was first physically realized at the nanoscale by Hewlett-Packard Labs,[2] it has become a core component in the hardware implementation of artificial neural networks due to its unique ability to mimic biological synaptic plasticity.[3,4] The introduction of memristors into neuronal dynamics frameworks enhances system nonlinearity,[5,6] owing to the compatibility between the unique physical properties of memristors and the functions of biological neurons. Specifically, their memory effect can simulate the dynamic firing behavior of ion channels in neurons,[7] while their variable resistance enables adaptive synaptic weight mechanisms.[8] These characteristics provide the foundation for constructing more complex neuron systems, whereas the practical application of such systems relies on digital simulation and hardware implementation.[9,10]

Compared with continuous memristive neuron systems, discrete memristive neuron maps (DMNMs) possess a simple structure, retain rich dynamical characteristics, and are more suitable for implementation in digital circuits.[11,12] To date, DMNMs have shown great potential in applications such as neural computation,[13,14] image encryption,[15] biomedical engineering,[16,17] and bio-inspired multimodal sensing circuits,[18] among others.

Although DMNMs have achieved considerable research progress in various applications, accurately identifying their parameters for control purposes remains a challenging task because of their unpredictability, strong nonlinearity, and sensitivity to initial conditions.[19] Intelligent optimization algorithms offer a promising solution by transforming the parameter identification problem into an optimization problem.[20] They can reduce dependence on initial values, lower the risk of identification failure caused by improper initialization, and ensure parameter identification accuracy to a certain extent.

Up to now, many intelligent optimization algorithms have been successfully applied to parameter identification in complex nonlinear systems. For example, Ebrahimi *et al.*[21] designed an improved chaotic optimization algorithm, which enhances the accuracy and robustness of parameter identification for complex nonlinear systems. In the field of mechanical modeling, Li *et al.*[22] investigated the influence of wolf pack number and iteration times on the parameter identification re-

†Corresponding author. E-mail: pyx244896301@163.com

© 2026 Chinese Physical Society and IOP Publishing Ltd. All rights, including for text and data mining, AI training, and similar technologies, are reserved.

sults of a magnetorheological damper mechanical model using an improved grey wolf algorithm. For electrical systems, Hu *et al.*[23] developed an enhanced raccoon optimization algorithm and successfully applied it to the electrical parameter identification of permanent magnet synchronous motors. For parameter identification in chaotic systems, Peng *et al.*[24] studied a fractional-order JAYA algorithm to identify parameters of four discrete chaotic maps, which exhibits high accuracy and stability. When addressing the parameter identification problem of fractional-order chaotic systems with more complex dynamical behaviors, some scholars have proposed the differential evolution algorithm,[25] an improved surrogate-assisted whale optimization algorithm,[26] a new state transition algorithm,[27] and other methods. These algorithms have provided valuable experience for parameter identification in such complex systems.

In recent years, memristive chaotic systems have garnered significant attention, and several scholars have attempted to utilize intelligent optimization algorithms for parameter identification to facilitate the control of these complex systems. For instance, Xiong *et al.*[28] proposed a new pelican optimization algorithm, which outperforms several traditional algorithms in terms of convergence speed and optimization accuracy. Similarly, Huang *et al.*[29] developed a brain-inspired state transition algorithm, providing a more effective and accurate solution for parameter identification. However, the aforementioned studies focus primarily on continuous memristive nonlinear systems, whereas research on parameter identification of discrete memristive systems remains relatively limited.

To sum up, there are three deficiencies in recent studies: (1) There is a lack of research on parameter identification of discrete memristive chaotic systems, especially DMNMs; (2) in-depth investigations into appropriate objective functions and optimal sample sizes are lacking, and the impacts of these factors on the accuracy and efficiency of parameter identification remain unclear; (3) existing intelligent optimization algorithms may not be well suited for DMNMs. Therefore, this paper focuses on the parameter identification problem of DMNMs. Recently, a new intelligent optimization algorithm called chaos game optimization (CGO)[30] has been developed and has demonstrated advantages such as strong global search capability and a simple structure compared with traditional algorithms. Therefore, the CGO algorithm is selected as the basis for parameter identification and further improved to enhance identification accuracy. In addition, this paper systematically investigates the impacts of sample size and objective function on identification performance.

The following are the primary contributions of this paper:

(1) The parameter identification problem of DMNMs is investigated to address the insufficient attention paid to parameter identification of DMNMs in the existing research on nonlinear systems.

(2) The effects of the objective function and sample size on identification performance are systematically explored, providing practical guidelines for parameter identification of DMNMs.

(3) A novel adaptive chaos game optimization (ACGO) algorithm is proposed to effectively escape local optima, thereby improving the accuracy and efficiency of parameter identification.

The rest of the paper is structured as follows. In Section 2, the principle of parameter identification is introduced. The design of the ACGO algorithm is detailed in Section 3. The experimental results are presented in Section 4. The conclusions and future research directions are given in Section 5.

2. Principle of parameter identification

Parameter identification for DMNMs is formulated as an optimization problem, and the principle of parameter identification is shown in Fig. 1.

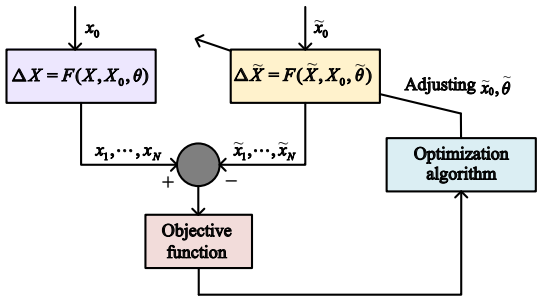


Fig. 1. The principle of parameter identification.

The specific details are as follows. First, consider a discrete memristive neuron map to be identified

$$\Delta \boldsymbol{X} = F(\boldsymbol{X}, \boldsymbol{X}_0, \boldsymbol{\theta}), \tag{1}$$

where $\boldsymbol{X} = (x_1, x_2, \ldots, x_N)^{\mathrm{T}} \in R^N$ is the state vector of the map, and N is its dimension. $\boldsymbol{X}_0$ denotes the initial state of the original system. $\boldsymbol{\theta} = (\theta_1, \theta_2, \ldots, \theta_D)^{\mathrm{T}} \in R^D$ represents the parameter vector of the original system, where D is the number of parameters to be identified.

If the structure of the original map is known, the identified map can be described as

$$\Delta \widetilde{\boldsymbol{X}} = F(\widetilde{\boldsymbol{X}}, \boldsymbol{X}_0, \widetilde{\boldsymbol{\theta}}), \tag{2}$$

where $\widetilde{\boldsymbol{X}} = (\tilde{x}_1, \tilde{x}_2, \ldots, \tilde{x}_N)^{\mathrm{T}} \in R^N$ is the N-dimensional state vector of the identified map, and $\widetilde{\boldsymbol{\theta}} = (\tilde{\theta}_1, \tilde{\theta}_2, \ldots, \tilde{\theta}_D)^{\mathrm{T}} \in R^D$ denotes the identified parameter vector.

Five different objective functions are employed in this study. The mathematical expressions of the mean squared error (MSE), mean absolute error (MAE), mean absolute percentage error (MAPE), median absolute error (MedAE), and root mean square error (RMSE) are given in Eqs. (3)–(7), respectively.

$$\mathrm{MSE} = \frac{1}{M} \sum_{k=1}^{M} \left(X_k - \tilde{X}_k \right)^2, \tag{3}$$

$$\mathrm{MAE} = \frac{1}{M}\sum_{k=1}^{M}\left|X_k - \tilde{X}_k\right|, \tag{4}$$

$$\mathrm{MAPE} = \frac{100\%}{M}\sum_{k=1}^{M}\left|\frac{X_k - \tilde{X}_k}{\tilde{X}_k}\right|, \tag{5}$$

$$\mathrm{MedAE} = \mathrm{median}(|X_1 - \tilde{X}_1|, |X_2 - \tilde{X}_2|, \ldots, |X_k - \tilde{X}_k|), \tag{6}$$

$$\mathrm{RMSE} = \sqrt{\frac{1}{M}\sum_{k=1}^{M}\left(X_k - \tilde{X}_k\right)^2}, \tag{7}$$

where M is the sample size, and median$(\cdot)$ denotes the median value.

3. Adaptive chaos game optimization algorithm

3.1. CGO algorithm

Chaos theory studies the behavior of dynamical systems, which are highly sensitive to initial conditions and exhibit seemingly random yet deterministic dynamics. Inspired by this theory, the CGO algorithm is a novel metaheuristic that incorporates the concepts of the chaos game and fractal self-similarity.[30] In this algorithm, the search process is optimized by simulating the chaos game in Sierpinski triangles with a fractal structure. Candidate solutions are treated as "seeds" within the fractal space, and their positions are dynamically updated according to transformation rules.

The initial positions of the candidate seeds are randomly determined within the search space:

$$x_i^j(0) = x_{i,\min}^j + \mathrm{rand}(x_{i,\max}^j - x_{i,\min}^j),$$
$$i = 1,2,\ldots,n,\quad j = 1,2,\ldots,d, \tag{8}$$

where $x_i^j(0)$ denotes the initial position of the i-th seed in the j-th dimension, and $x_{i,\min}^j$ and $x_{i,\max}^j$ are the minimum and maximum allowable values for the j-th decision variable of the i-th candidate solution. Here, n is the total number of candidate solutions, and d is the problem dimension. The term rand is a uniformly distributed random number in $[0,1]$.

The creation of temporary triangles aims to generate new candidate seeds in the search space. The update of $\mathrm{Seed}_i^1(t+1)$ is defined as

$$\mathrm{Seed}_i^1(t+1) = X_i(t) + \alpha_i \times (\beta_i \times GB(t) - \gamma_i \times MG_i(t)),$$
$$i = 1,2,\ldots,n, \tag{9}$$

where $X_i(t)$ is the i-th candidate solution at iteration t, and $GB(t)$ is the current global best solution. α_i is the movement limitation factor. β_i and γ_i are random vectors with entries in [0, 1]. $MG_i(t)$ is the mean of randomly selected seeds at iteration t.

The update of $\mathrm{Seed}_i^2(t+1)$ is given by

$$\mathrm{Seed}_i^2(t+1) = GB(t) + \alpha_i \times (\beta_i \times X_i(t) - \gamma_i \times MG_i(t)),$$
$$i = 1,2,\ldots,n. \tag{10}$$

The update of $\mathrm{Seed}_i^3(t+1)$ is defined as

$$\mathrm{Seed}_i^3(t+1) = MG_i(t) + \alpha_i \times (\beta_i \times X_i(t) - \gamma_i \times GB(t)),$$
$$i = 1,2,\ldots,n. \tag{11}$$

The fourth seed is updated via random perturbations of decision variables using

$$\mathrm{Seed}_i^4(t+1) = X_i(x_i^k(t) = x_i^k(t) + \mathrm{rand}),$$
$$k = 1,2,\ldots,d, \tag{12}$$

where k is a randomly selected integer in [1, d].

The movement limitation factor α_i is determined by four possible scenarios:

$$\alpha_i = \begin{cases} \mathrm{rand}, \\ 2 \times \mathrm{rand}, \\ (\delta \times \mathrm{rand}) + 1, \\ (\delta \times \mathrm{rand}) + (1 - \delta), \end{cases} \tag{13}$$

where δ is either 0 or 1.

In CGO, the fitness of newly generated seeds is compared with existing seeds, and the better seeds are retained.

3.2. The ACGO algorithm

To enhance the performance of CGO for parameter identification, the ACGO algorithm integrates a differential evolution mutation strategy and a Cauchy adaptive parameter mechanism to overcome the limitations of the classical CGO.

3.2.1. Differential evolution mutation strategy

In the original CGO, the fourth seed is generated randomly, lacking directional guidance and reducing local search capability. To address this, the fourth seed update is improved by incorporating the differential evolution mutation principle. The updated formula is

$$\mathrm{Seed}_i^4(t+1) = X_i^{r1}(t) + F_i \times \left(X_i^{r2}(t) - X_i^{r3}(t)\right), \tag{14}$$

where F_i is the scaling factor of the i-th candidate solution, and $X_i^{r1}(t)$, $X_i^{r2}(t)$, $X_i^{r3}(t)$ are three distinct seeds randomly selected from the population at iteration t.[31]

3.2.2. Cauchy adaptive parameter mechanism

The scaling factor F_i significantly affects the search efficiency. ACGO uses the Cauchy adaptive parameter mechanism from the JADE algorithm[32] to adjust F_i dynamically. The mechanism records F_i of successfully mutated candidates, computes the Lehmer mean to update the location parameter u_{F}, and generates new F_i values conforming to a Cauchy distribution

$$F_i = \max\left(u_{\mathrm{F}} + \gamma \times \tan(\pi \times (\mathrm{rand} - 0.5)),\ 0.1\right), \tag{15}$$

where γ is a scale parameter. The max function ensures $F_i \geq 0.1$.

The location parameter u_{F} is updated as

$$u_{\mathrm{F}} = (1-c) \times u_{\mathrm{F}} + c \times \mathrm{mean}_{\mathrm{L}}(S_{\mathrm{F}}), \tag{16}$$

where S_{F} is the set of scaling factors for successfully mutated candidates, $c \in [0,1]$, and $\mathrm{mean}_{\mathrm{L}}(\cdot)$ denotes the Lehmer mean

$$\mathrm{mean}_{\mathrm{L}}(S_{\mathrm{F}}) = \frac{\sum\limits_{F_i \in S_{\mathrm{F}}} F_i^2}{\sum\limits_{F_i \in S_{\mathrm{F}}} F_i}. \tag{17}$$

The pseudo-code of the ACGO algorithm is presented in Algorithm 1, and the flowchart is shown in Fig. 2.

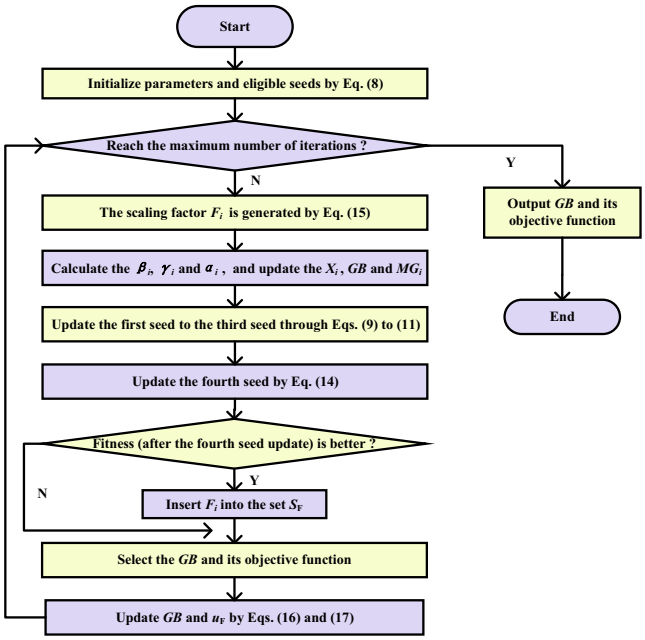


Fig. 2. The flowchart of the ACGO algorithm.

Algorithm 1 Pseudo-code of ACGO.

Input: candidate solutions' size n, the lower and upper limit of decision variable $x_{\min}$ and $x_{\max}$, dimension of problem d and the maximum of iterations maxgen.

Output: GB and its objective function.

Set the initial values of u_{F}, γ and c
Eligible seeds are initialized by Eq. (8)
for $i = 1, 2, \ldots,$ maxgen **do**
    The scaling factor F_i is generated by Eq. (15)
    Update the GB and its objective function
    for $j = 1, 2, \cdots, n$ **do**
        Update the X_i, GB and MG_i
        Calculate the β_i, γ_i and α_i
        Update the first seed to the third seed through Eqs. (9) to (11)
        Update the fourth seed by Eq. (14)
        if fitness (the fourth seed update) > fitness (before) **then**
            $F_i \rightarrow S_{\mathrm{F}}$
        end if
        Select GB and its objective function
        Update u_{F} by Eqs. (16) and (17)
    end for
end for

3.3. Time complexity analysis

To evaluate the computational efficiency of ACGO and its feasibility in practical applications, a time complexity analysis is conducted for both CGO and ACGO. Let maxgen denote the maximum number of iterations, n the population size, and d the problem dimension. The computational cost of CGO mainly consists of initialization, position updates, and sorting operations; thus, its time complexity is $O(\mathrm{maxgen} \cdot (n \cdot d + n \log n))$. Although ACGO integrates the differential evolution mutation strategy and the Cauchy adaptive parameter mechanism, these two strategies only introduce linear-level overheads of $O(n)$ and $O(d)$, respectively. Therefore, the overall time complexity of ACGO remains $O(\mathrm{maxgen} \cdot (n \cdot d + n \log n))$, which is consistent with that of CGO.

4. Numerical simulations

To demonstrate the performance and engineering applicability of the ACGO algorithm, it is compared with seven typical intelligent optimization algorithms, including the CGO algorithm,[30] DE algorithm,[33] FODE algorithm,[34] GWO algorithm,[35] MPA algorithm,[36] PSO algorithm,[37] and SCSO algorithm,[38] for parameter identification of five discrete memristive neuron maps (DMNMs). Meanwhile, the performance of these algorithms under five objective functions, as well as the performance of the ACGO algorithm under different sample sizes, is also compared to obtain more comprehensive results. Experiments were conducted on an Intel(R) Core(TM) i7-14650HX CPU @ 2.2 GHz with 16 GB RAM, running Windows 11 and MATLAB 2022b.

The maximum number of iterations for each algorithm was set to maxgen = 500, and the population size was set to PopSize = 40. Other parameter settings are presented in Table 1. To eliminate randomness, 50 independent runs were performed for each algorithm. Generally, the smaller the objective function value J, the higher the identification accuracy. When the error between each identified parameter and the corresponding true parameter is less than 1×10^{-4}, the identification is considered accurate (Acc).

Table 1. Parameter settings of intelligent optimization algorithms.

Algorithm	Parameter setting
ACGO	$u_{\mathrm{F}} = 0.5$, $\gamma = 0.1$, $c = 0.1$
CGO	No specific parameters
DE	$F = 0.4$, CR $= 0.1$
FODE	$F = 0.8$, Cr $= 0.9$, $f_\mathrm{rate} = 0.1$, MemorySize $= 6$, archiveSize $= 1.5$, $p_\mathrm{best_rate} = 0.1$
GWO	No specific parameters
MPA	FADs $= 0.2$, P $= 0.5$
PSO	$c_1 = c_2 = 0.5$, $\omega_{\max} = 0.9$, $\omega_{\min} = 0.4$
SCSO	$S = 2$

4.1. Identified discrete memristive neuron maps

4.1.1. Memristive Rulkov neuron map (MRNM)

The MRNM equation is given as[39]

$$\begin{cases} x_{n+1} = F(x_n, y_n) + k\tanh(z_n)x_n, \\ y_{n+1} = y_n - ax_n, \\ z_{n+1} = z_n + bx_n, \end{cases} \tag{18}$$

where a, b, and k are control parameters. $F(x,y)$ is a nonlinear discontinuous function defined as

$$F(x,y) = \begin{cases} \alpha/(1-x)+y, & x \le 0, \\ \alpha + y, & 0 < x < \alpha + y, \\ -1, & x \ge \alpha + y, \end{cases} \tag{19}$$

where α is a control parameter and is fixed as $\alpha = 5$.

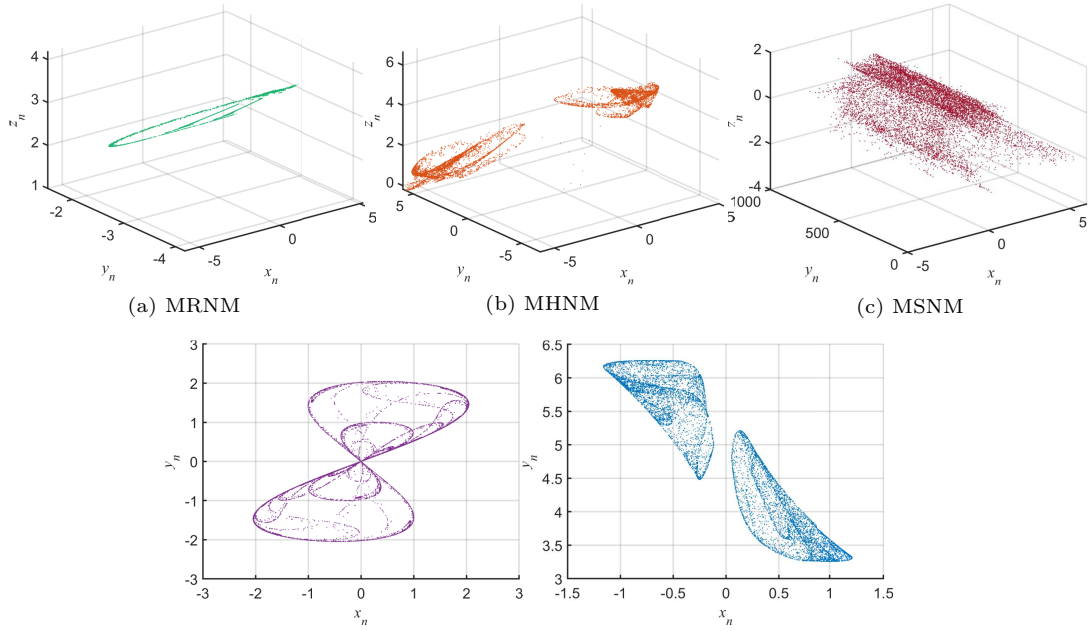
When the parameters of the system (18) are set to $a = 0.05$, $b = 0.05$, $k = 0.55$, $x_0 = 0$, $y_0 = 0$, and $z_0 = 0$, the system exhibits chaotic behavior, with the largest Lyapunov exponent equal to 0.0414. The attractor phase diagram is shown in Fig. 3(a).

4.1.2. Memristive Hénon neuron map (MHNM)

The equation of MHNM is defined as[40]

$$\begin{cases} x_{n+1} = 1 - ax_n^2 + y_n, \\ y_{n+1} = bx_n + ky_n\tanh(z_n), \\ z_{n+1} = y_n + z_n, \end{cases} \tag{20}$$

where a, b, and k are the control parameters. When the parameters of system (20) are fixed to $a = 0.25$, $b = 0.51$, $k = -0.89$, $x_0 = 0$, $y_0 = 0$, $z_0 = 0$, it enters a chaotic state, with the largest Lyapunov exponent of 0.1309, and the attractor phase diagram is displayed in Fig. 3(b).



(a) MRNM (b) MHNM (c) MSNM

(d) MCM (e) MCNM

Fig. 3. Chaotic attractors of five DMNMs.

4.1.3. Memristive synapse neuron map (MSNM)

The MSNM is described as[41]

$$\begin{cases} x_{n+1} = \dfrac{a}{1+x_n^2} + b + k\big(c + d\sin(y_n)\big)z_n, \\ y_{n+1} = y_n + ez_n, \\ z_{n+1} = z_n + ex_n, \end{cases} \tag{21}$$

where a, b, c, d, e, and k are the control parameters. a is fixed as 4.1, b as -2, and c as -8. When the parameters of system (21) are set to $e = 0.5$, $d = 0.8$, $k = 0.2$, $x_0 = -0.1$, $y_0 = -0.1$, $z_0 = 0.2$, it enters a hyperchaotic state, with Lyapunov exponents of 0.4573 and 0.0123. The hyperchaotic attractor phase diagram is presented in Fig. 3(c).

4.1.4. Memristive chaotic map (MCM)

The MCM equation is depicted as[42]

$$\begin{cases} x_{n+1} = ax_n\cos(y_n), \\ y_{n+1} = bx_n, \end{cases} \tag{22}$$

where a and b are the control parameters. When the parameters of system (22) are set to $a = 2$, $b = 1$, $x_0 = 0.001$, $y_0 = 0.001$, it enters a chaotic state, with a largest Lyapunov exponent of 0.3357, and the attractor phase diagram is displayed in Fig. 3(d).

4.1.5. Memristive Chialvo neuron map (MCNM)

The MCNM's equation is expressed as[43]

$$\begin{cases} x_{n+1} = x_n^2 e^{a-x_n} + k\sin(y_n)x_n, \\ y_{n+1} = y_n + b\tanh(x_n), \end{cases} \tag{23}$$

where a, b, and k are the control parameters. When the parameters of system (23) are fixed to $a = -2.5$, $b = 3.5$, $k = 2.15$, $x_0 = 0.001$, $y_0 = 0.5$, it enters a hyperchaotic state, with Lyapunov exponents of 0.2237 and 0.0245. The hyperchaotic attractor phase diagram is shown in Fig. 3(e).

Subsequent experiments use the parameter settings shown in Fig. 3 as the parameters to be identified. Specifically, for MRNM, the parameters to be identified are $a = 0.05$, $b = 0.05$, $k = 0.55$, $x_0 = 0$, $y_0 = 0$; for MHNM, $a = 0.25$, $b = 0.51$, $k = -0.89$, $x_0 = 0$, $y_0 = 0$; for MSNM, $e = 0.5$, $d = 0.8$, $k = 0.2$, $y_0 = -0.1$, $z_0 = 0.2$; for MCM, $a = 2$, $b = 1$, $x_0 = 0.001$, $y_0 = 0.001$; and for MCNM, $a = -2.5$, $b = 3.5$, $k = 2.15$, $x_0 = 0.001$, $y_0 = 0.5$.

4.2. Effect of sample size on parameter identification

The sample size influences identification efficiency. A smaller sample size often yields higher efficiency and accuracy, whereas an excessively large sample size may increase information redundancy and computational complexity.[44] To verify the robustness of the algorithm under small-sample conditions and to determine the appropriate sample size, the sample sizes were set to 3, 4, 5, 7, and 10. In these experiments, the objective function was selected as the MSE, and the ACGO algorithm was used for parameter identification of the five DMNMs. Simulation results of the ACGO algorithm for parameter identification with different sample sizes M are presented in Table 2. It can be observed that MRNM, MHNM, and MSNM achieve close to 100% identification accuracy across most sample sizes. In contrast, MCM and MCNM perform less accurately but can still be successfully identified. Moreover, increasing the sample size generally leads to a decrease in identification accuracy and the mean J value. Notably, the identification accuracy of MHNM is 0% for sample size $M = 3$ due to the multistability of this map. Different initial values can produce nearly identical dynamic behaviors in the early stages, making it difficult to distinguish between sequence errors with limited samples.[45] Although optimal or near-optimal identification accuracy is observed when the sample size is $M = 3$ or $M = 4$ for most DMNMs, $M = 3$ is unstable and fails for MHNM. Considering both accuracy and stability, a sample size of $M = 4$ is recommended.

Table 2. Identification results for different sample sizes in five DMNMs.

DMNMs	M	3	4	5	7	10
MRNM	*Acc* (%)	**100%**	**100%**	96%	98%	92%
	Mean J	1.4475e-141	7.7640e-146	5.5071e-03	5.2530e-03	5.3713e-02
MHNM	*Acc* (%)	0%	**100%**	**100%**	**100%**	**100%**
	Mean J	**1.0734e-190**	2.3417e-175	1.2749e-149	5.9453e-155	3.1271e-147
MSNM	*Acc* (%)	**100%**	**100%**	98%	**100%**	**100%**
	Mean J	7.0874e-34	**0**	2.5030e-02	1.0420e-32	3.3099e-02
MCM	*Acc* (%)	**84%**	**84%**	62%	30%	0%
	Mean J	1.6452e-07	**1.5258e-07**	3.3426e-07	5.1135e-07	3.4077e-07
MCNM	*Acc* (%)	14%	**34%**	18%	10%	**22%**
	Mean J	**1.3003e-06**	2.6909e-06	3.9249e-06	1.2679e-05	2.5628e-05

4.3. Impact of different objective functions on parameter identification

The objective function directly determines how the optimization algorithm evaluates the results. Its selection affects both the performance of the optimization algorithm and its suitability for a given application scenario. In these experiments, five objective functions were employed, namely MSE, MAE, MAPE, MedAE, and RMSE (Eqs. (3)–(7)). The sample size was set as $M = 4$, and parameters of five DMNMs were identified using eight algorithms.

The simulation results for the MRNM are presented in Table 3, including the identification accuracy (*Acc*), the best, mean, and median values of the objective function J, as well as the specific parameter identification results. The ACGO, CGO, FODE, and MPA algorithms all exhibit high identification accuracy. Notably, only ACGO and MPA achieve 100% *Acc* across all objective functions. Furthermore, ACGO attains lower values of the objective function J than MPA, indicating superior performance in the parameter identification of MRNM. The convergence curves for these eight intelligent optimization algorithms under the five objective functions are illustrated in Fig. 4. It can be observed that the fitness values of all algorithms gradually decrease as the number of iterations increases. Meanwhile, ACGO demonstrates the fastest convergence among all objective functions, followed by CGO, with FODE ranking third. The remaining algorithms exhibit steady-state convergence.

The parameter identification results for the MHNM are summarized in Table 4. As presented, ACGO, CGO, FODE, and MPA achieve 100% identification accuracy across all objective functions except MedAE. In contrast, GWO and PSO reach near-100% accuracy only under the MSE objective function, highlighting the effectiveness of MSE for parameter identification of MHNM. The corresponding convergence curves are shown in Fig. 5. Similar to Fig. 4, ACGO exhibits the fastest convergence rate, followed by CGO. FODE ranks third for MAE, MAPE, and MedAE, while PSO ranks third for MSE and RMSE.

Table 3. Statistical results of parameter identification on MRNM under five objective functions.

Algorithm	J	Acc (%)	Best J	Mean J	Median J	$a = 0.05$	$b = 0.05$	$k = 0.55$	$x_0 = 0$	$y_0 = 0$
ACGO	MSE	**100%**	3.6167e-159	7.7640e-146	2.0885e-152	5.0000e-02	5.0000e-02	5.5000e-01	−1.2543e-77	−6.7233e-80
	MAE	**100%**	5.6797e-77	5.5511e-19	1.7522e-73	5.0000e-02	5.0000e-02	5.5000e-01	4.4349e-75	2.2719e-76
	MAPE	**100%**	5.0000e-01	5.0000e-01	5.0000e-01	5.0000e-02	5.5000e-02	5.5000e-01	4.4325e-16	8.0272e-17
	MedAE	**100%**	0	2.4980e-16	3.5284e-111	5.0000e-02	5.0000e-02	5.5000e-01	8.1473e-112	8.8300e-18
	RMSE	**100%**	1.4128e-78	2.5170e-73	1.4840e-74	5.0000e-02	5.0000e-02	5.5000e-01	4.7531e-76	2.1060e-76
CGO	MSE	**100%**	3.6875e-92	3.5633e-83	1.8666e-86	5.0000e-02	5.0000e-02	5.5000e-01	1.2509e-44	3.2800e-46
	MAE	**100%**	2.2206e-45	1.1102e-18	1.9304e-43	5.0000e-02	5.0000e-02	5.5000e-01	8.7083e-43	3.7426e-44
	MAPE	**100%**	5.0000e-01	5.0000e-01	5.0000e-01	5.0000e-02	5.0000e-02	5.5000e-01	4.8615e-16	7.8117e-17
	MedAE	98%	3.0279e-75	1.2993e-05	8.1831e-28	5.0000e-02	5.0000e-02	5.5000e-01	1.4596e-58	1.0637E-16
	RMSE	**100%**	1.8358e-46	8.7771e-19	1.0030e-43	5.0000e-02	5.0000e-02	5.5000e-01	6.5449e-44	1.7769e-44
DE	MSE	86%	2.9961e-15	8.7129e-06	2.3855e-11	5.0000e-02	5.0000e-02	5.5000e-01	1.7898e-05	−3.1357e-08
	MAE	**100%**	4.0543e-07	2.6821e-05	2.9920e-06	5.0000e-02	5.0000e-02	5.5000e-01	2.9822e-06	8.1899e-08
	MAPE	0%	5.0311e-01	5.1786e-01	5.1435e-01	4.9435e-02	5.0096e-02	5.5628e-01	4.0254e-02	3.1441e-03
	MedAE	0%	1.2354e-03	5.1644e-03	4.6194e-03	4.9510e-02	4.9628e-02	5.1139e-01	2.9885e-02	6.8575e-04
	RMSE	88%	6.1289e-07	4.6226e-04	2.0325e-06	5.0000e-02	5.0000e-02	5.5000e-01	6.0110e-06	7.8227e-08
FODE	MSE	94%	4.1078e-87	2.5410e-01	2.8371e-77	5.0000e-02	5.0000e-02	5.5000e-01	−1.2979e-40	1.1930e-41
	MAE	84%	2.2936e-43	3.4239e-01	2.0968e-37	5.0000e-02	5.0000e-02	5.5000e-01	−4.2324e-38	−4.5629e-39
	MAPE	**96%**	5.0000e-01	5.4753e-01	5.0000e-01	5.0000e-02	5.0000e-02	5.5000e-01	5.2250e-16	8.6263e-17
	MedAE	90%	0	2.0169e-02	3.4672e-34	5.0000e-02	5.0000e-02	5.5000e-01	2.7343e-33	6.8911e-18
	RMSE	82%	1.0822e-42	3.4184e-01	1.8965e-36	5.0000e-02	5.0000e-02	5.5000e-01	−1.3864e-39	1.1237e-38
GWO	MSE	0%	5.2961e-08	9.6152e-01	1.3586e-05	4.9763e-02	4.9670e-02	5.5438e-01	1.3979e-02	1.8729e-03
	MAE	0%	7.3257e-04	5.9684e-01	4.9033e-03	4.9716e-02	4.9813e-02	5.4888e-01	2.1441e-02	9.8644e-04
	MAPE	0%	5.0135e-01	5.7770e-01	5.3385e-01	4.8404e-02	4.8494e-02	7.7145e-02	1.4050e-01	3.0302E-03
	MedAE	0%	1.0293e-03	7.2105e-03	8.0625e-03	4.9438e-02	4.9603e-02	3.7751e-02	4.3752e-02	4.9756E-04
	RMSE	0%	7.1269e-04	2.5276e-01	3.5786e-03	4.9728e-02	4.9968e-02	5.5474e-01	2.1301e-00	1.7360e-03
MPA	MSE	**100%**	1.2150e-15	1.5800e-13	5.2241e-14	5.0000e-02	5.0000e-02	5.5000e-01	1.6987e-06	4.7776e-08
	MAE	**100%**	1.4098e-07	6.2302e-07	5.3975e-07	5.0000e-02	5.0000e-02	5.5000e-01	3.0778e-06	6.9197e-08
	MAPE	**100%**	5.0000e-01	5.0000e-01	5.0000e-01	5.0000e-02	5.0000e-02	5.5000e-01	7.1738e-06	9.4732e-08
	MedAE	**100%**	2.6041e-07	1.1778e-06	1.0418e-06	5.0000e-02	5.0000e-02	5.5000e-01	1.5052e-05	5.1899e-07
	RMSE	**100%**	7.8122e-08	4.1175e-07	2.9664e-07	5.0000e-02	5.0000e-02	5.5000e-01	1.9083e-06	7.9835e-09
PSO	MSE	**2%**	5.8732e-26	5.5553e-01	9.1798e-03	4.6356e-02	4.8045e-02	5.1793e-01	1.3059e-01	1.2974e-02
	MAE	0%	2.5099e-02	9.0766e-01	2.8005e-01	3.8386e-02	4.5840e-02	−1.7541e-02	1.7644e-01	1.9596E-03
	MAPE	0%	5.2017e-01	9.0704e-01	6.8743e-01	4.2014e-02	4.7433e-02	2.0334e-03	4.7530e-01	2.9083e-02
	MedAE	0%	4.2354e-04	3.3079e-01	3.3391e-01	3.6239e-02	3.9405e-02	2.6661e-18	−5.7935e-02	−1.7676e-16
	RMSE	0%	1.7265e-03	3.6100e-01	1.0848e-01	4.2609e-02	4.9279e-02	5.1543e-01	1.6342e-01	1.2947e-02
SCSO	MSE	0%	1.8052e-06	1.0018e-05	9.8055e-06	4.9784e-02	4.9703e-02	5.5417e-01	2.0276e-02	−1.5500e-03
	MAE	0%	6.1409e-04	1.1986e-01	5.1923e-03	4.9744e-02	4.9999e-02	5.4820e-01	2.4425e-02	1.0555e-03
	MAPE	0%	5.0312e-01	5.2748e-01	5.3433e-01	4.8896e-02	4.7697e-02	3.1409e-02	9.8801e-02	−1.8697e-03
	MedAE	0%	1.3051e-03	7.8166e-03	7.6302e-03	4.9110e-02	4.9532e-02	2.9822e-03	4.3538e-02	7.1927e-04
	RMSE	0%	8.8478e-04	2.9693e-03	3.0637e-03	4.9830e-02	4.9516e-02	5.5402e-01	1.7126e-02	−2.4789e-03

Table 4. Statistical results of parameter identification on MHNM under five objective functions.

Algorithm	J	Acc (%)	Best J	Mean J	Median J	$a = 0.25$	$b = 0.51$	$k = -0.89$	$x_0 = 0$	$y_0 = 0$
ACGO	MSE	**100%**	8.6714e-186	2.3417e-175	5.6459e-180	2.5000e-01	5.1000e-01	−8.9000e-01	−2.0570e-92	6.5859e-92
	MAE	**100%**	4.4629e-91	3.9868e-87	7.1953e-88	2.5000e-01	5.1000e-01	−8.9000e-01	1.3651e-90	−3.6997e-90
	MAPE	**100%**	7.5000e-01	7.5000e-01	7.5000e-01	2.5000e-01	5.1000e-01	−8.9000e-01	−1.5392e-17	3.7740e-17
	MedAE	0%	5.9031e-170	7.2019e-155	2.9603e-161	2.5000e-01	5.1000e-01	4.7941e-02	−4.2668e-164	−2.1343e-164
	RMSE	**100%**	4.0676e-91	2.0009e-85	9.6796e-88	2.5000e-01	5.1000e-01	−8.9000e-01	−6.4206e-90	−1.4226e-89
CGO	MSE	**100%**	4.8412e-122	5.7912e-113	1.5689e-117	2.5000e-01	5.1000e-01	−8.9000e-01	3.4296e-60	−3.4541e-61
	MAE	**100%**	4.1835e-62	4.1655e-58	1.7278e-59	2.5000e-01	5.1000e-01	−8.9000e-01	−2.0455e-61	−5.8798e-61
	MAPE	**100%**	7.5000e-01	7.5000e-01	7.5000e-01	2.5000e-01	5.1000e-01	−8.9000e-01	−6.8941e-17	3.0407e-17
	MedAE	0%	1.6666e-113	3.3010e-80	2.8366e-105	2.5000e-01	5.1000e-01	−5.7147e-01	−5.3991e-111	−3.2684e-109
	RMSE	**100%**	2.0884e-62	4.8540e-58	3.2958e-59	2.5000e-01	5.1000e-01	−8.9000e-01	1.3207e-60	−3.5308e-61

Table 4. Continued.

Algorithm	J	*Acc* (%)	Best J	Mean J	Median J	$a = 0.25$	$b = 0.51$	$k = -0.89$	$x_0 = 0$	$y_0 = 0$
DE	MSE	84%	3.4698e-07	2.0330e-16	3.7918e-11	2.4999e-01	5.1000e-01	−8.8998e-01	−2.7591e-06	4.6138e-06
	MAE	**100%**	3.9148e-07	4.0003e-06	9.0308e-07	2.5000e-01	5.1000e-01	−8.9000e-01	−1.8211e-07	8.7641e-08
	MAPE	2%	7.5050e-01	7.5716e-01	7.5508e-01	2.4991e-01	5.0979e-01	−8.8628e-01	1.2015e-03	2.6020e-04
	MedAE	0%	5.3974e-06	8.5983e-04	3.0941e-04	2.4999e-01	5.1000e-01	−6.9235e-01	−3.8191e-06	3.5693e-06
	RMSE	68%	4.5998e-07	6.6202e-04	3.8935e-05	2.4996e-01	5.0998e-01	−8.8991e-01	−3.1983e-05	3.1655e-05
FODE	MSE	**100%**	1.0997e-98	2.1775e-77	2.6981e-88	2.5000e-01	5.1000e-01	−8.9000e-01	−2.1188e-45	1.7603e-46
	MAE	**100%**	2.0616e-48	1.4648e-41	4.5203e-45	2.5000e-01	5.1000e-01	−8.9000e-01	5.8810e-48	3.3216e-48
	MAPE	**100%**	7.5000e-01	7.5000e-01	7.5000e-01	2.5000e-01	5.1000e-01	−8.9000e-01	−4.4276e-18	2.8789e-17
	MedAE	0%	1.1294e-68	1.7775e-53	2.1113e-61	2.5000e-01	5.1000e-01	−6.4476e-01	−1.6220e-65	5.7047e-61
	RMSE	**100%**	9.6447e-50	7.8291e-41	4.7635e-44	2.5000e-01	5.1000e-01	−8.9000e-01	−1.2226e-48	5.7906e-49
GWO	MSE	**100%**	7.2598e-07	8.5924e-05	1.2767e-05	2.4995e-01	5.0946e-01	−8.8911e-01	1.4037e-03	6.2589e-04
	MAE	0%	3.6627e-04	9.0270e-03	3.8925e-03	2.5013e-01	5.0991e-01	−8.8840e-01	5.3255e-04	−1.1080e-04
	MAPE	0%	7.5109e-01	7.6757e-01	7.5547e-01	2.4847e-01	5.0886e-01	−8.8151e-01	−1.4971e-03	2.4168e-03
	MedAE	0%	9.2967e-04	3.8588e-03	3.2374e-03	2.4995e-01	5.1029e-01	−5.5485e-01	−1.0903e-03	−7.4643e-05
	RMSE	0%	4.5846e-04	4.0508e-03	4.1119e-03	2.4935e-01	5.0928e-01	−8.8734e-01	−1.4096e-04	1.1705e-03
MPA	MSE	**100%**	1.0794e-17	3.8357e-16	2.2902e-16	2.5000e-01	5.1000e-01	−8.9000e-01	−6.6566e-09	1.7168e-09
	MAE	**100%**	2.0078e-08	6.5037e-08	5.9448e-08	2.5000e-01	5.1000e-01	−8.9000e-01	−5.3378e-09	−4.5968e-09
	MAPE	**100%**	7.5000e-01	7.5000e-01	7.5000e-01	2.5000e-01	5.1000e-01	−8.9000e-01	4.7991e-08	−1.2452e-08
	MedAE	0%	6.7821e-08	3.5385e-07	2.5572e-07	2.5000e-01	5.1000e-01	−6.2880e-01	2.2569e-08	−9.6481e-09
	RMSE	**100%**	6.8398e-09	2.3475e-08	2.3218e-08	2.5000e-01	5.1000e-01	−8.9000e-01	5.4715e-09	−6.9109e-10
PSO	MSE	**92%**	2.2196e-102	2.2594e-05	1.0670e-98	2.5000e-01	5.1000e-01	−8.9000e-01	2.0501e-50	5.1073e-51
	MAE	0%	8.8359e-04	6.3485e-02	6.3181e-02	2.5000e-01	5.1000e-01	3.9278e-01	1.8084e-18	−9.5259e-20
	MAPE	0%	7.5746e-01	8.6518e-01	8.2709e-01	2.5000e-01	5.1000e-01	1.1443e-01	1.0168e-16	9.6372e-17
	MedAE	0%	8.2591e-54	7.1796e-02	1.7437e-02	2.5004e-01	5.1000e-01	−4.6973e-03	1.2706e-04	6.7210e-06
	RMSE	80%	5.1167e-51	9.2509e-03	1.0312e-49	2.5000e-01	5.1000e-01	−8.9000e-01	1.5999e-50	−1.4382e-51
SCSO	MSE	0%	6.3256e-07	5.5471e-04	1.9258e-05	2.4868e-01	5.0910e-01	−8.8490e-01	1.8283e-03	2.0764e-03
	MAE	0%	1.7622e-04	1.3509e-02	6.6717e-03	2.5017e-01	5.0934e-01	−8.7854e-01	1.5777e-03	−2.4196e-04
	MAPE	0%	7.5242e-01	7.7460e-01	7.6041e-01	2.4900e-01	5.0862e-01	−8.7666e-01	2.7924e-04	2.7543e-03
	MedAE	0%	5.5506e-04	7.5435e-03	6.8633e-03	2.4887e-01	5.0886e-01	−8.8395e-01	−2.6878e-04	2.2038e-03
	RMSE	0%	2.2102e-03	9.7233e-03	4.4196e-03	2.4963e-01	5.1075e-01	−1.1055e-01	−2.0614e-03	7.2799e-04

Table 5. Statistical results of parameter identification on MSNM under five objective functions.

Algorithm	J	*Acc* (%)	Best J	Mean J	Median J	$e = 0.5$	$d = 0.8$	$k = 0.2$	$y_0 = -0.1$	$z_0 = 0.2$
ACGO	MSE	**100%**	0	0	0	5.0000e-01	8.0000e-01	2.0000e-01	−1.0000e-01	2.0000e-01
	MAE	**100%**	0	7.7022e-18	0	5.0000e-01	8.0000e-01	2.0000e-01	−1.0000e-01	2.0000e-01
	MAPE	**100%**	2.5000e-01	2.5000e-01	2.5000e-01	5.0000e-01	8.0000e-01	2.0000e-01	−1.0000e-01	2.0000e-01
	MedAE	86%	0	5.3757e-05	0	5.0000e-01	8.0000e-01	2.0000e-01	−1.0000e-01	2.0000e-01
	RMSE	**100%**	0	0	0	5.0000e-01	8.0000e-01	2.0000e-01	−1.0000e-01	2.0000e-01
CGO	MSE	**100%**	0	1.9664e-33	0	5.0000e-01	8.0000e-01	2.0000e-01	−1.0000e-01	2.0000e-01
	MAE	**100%**	0	1.8804e-17	0	5.0000e-01	8.0000e-01	2.0000e-01	−1.0000e-01	2.0000e-01
	MAPE	**100%**	2.5000e-01	2.5000e-01	2.5000e-01	5.0000e-01	8.0000e-01	2.0000e-01	−1.0000e-01	2.0000e-01
	MedAE	78%	0	1.0084e-04	1.3878e-17	5.0000e-01	8.0000e-01	2.0000e-01	−1.0000e-01	2.0000e-01
	RMSE	**100%**	0	1.2443e-17	0	5.0000e-01	8.0000e-01	2.0000e-01	−1.0000e-01	2.0000e-01
DE	MSE	0%	1.0002e-06	6.6009e-06	1.4302e-06	4.9993e-01	8.1339e-01	2.0009e-01	−9.9515e-02	1.9948e-01
	MAE	**68%**	8.9900e-07	5.3691e-05	7.8621e-06	5.0000e-01	8.0002e-01	2.0000e-01	−9.9999e-02	2.0000e-01
	MAPE	20%	2.5002e-01	2.5142e-01	2.5031e-01	5.0000e-01	7.9972e-01	1.9999e-01	−9.9986e-02	2.0000e-01
	MedAE	0%	1.6546e-04	1.3509e-03	1.0246e-03	4.9997e-01	7.8806e-01	1.9994e-01	−1.0001e-01	2.0015e-01
	RMSE	42%	8.6290e-06	7.2047e-04	1.0809e-04	4.9999e-01	8.0045e-01	2.0000e-01	−9.9978e-02	1.9999e-01
FODE	MSE	**100%**	0	0	0	5.0000e-01	8.0000e-01	2.0000e-01	−1.0000e-01	2.0000e-01
	MAE	96%	0	4.1736e-02	0	5.0000e-01	8.0000e-01	2.0000e-01	−1.0000e-01	2.0000e-01
	MAPE	94%	2.5000e-01	3.2497e-01	2.5000e-01	5.0000e-01	8.0000e-01	2.0000e-01	−1.0000e-01	2.0000e-01
	MedAE	88%	0	1.6698e-05	0	5.0000e-01	8.0000e-01	2.0000e-01	−1.0000e-01	2.0000e-01
	RMSE	**100%**	0	0	0	5.0000e-01	8.0000e-01	2.0000e-01	−1.0000e-01	2.0000e-01

Table 5. Continued.

Algorithm	J	*Acc* (%)	Best J	Mean J	Median J	$e = 0.5$	$d = 0.8$	$k = 0.2$	$y_0 = -0.1$	$z_0 = 0.2$
GWO	MSE	0%	2.5527e-07	1.7314e-01	6.2387e-04	4.9778e-01	−5.9428e-02	1.9607e-01	−8.1612e-02	1.9277e-01
	MAE	0%	8.1696e-04	9.5347e-02	8.1696e-04	4.9812e-01	6.1968e-01	2.0049e-01	−9.9129e-02	1.9908e-01
	MAPE	0%	2.5176e-01	4.7039e-01	2.6418e-01	4.9874e-01	4.3168e-02	1.9814e-01	−9.9398e-02	2.0011e-01
	MedAE	0%	4.7685e-04	2.3105e-02	6.7152e-03	4.9810e-01	6.1276e-02	1.9838e-01	−9.7093e-02	2.0056e-01
	RMSE	0%	1.2828e-03	1.4011e-01	2.1051e-02	4.9855e-01	1.7405e-02	1.9611e-01	−9.9829e-02	2.0080e-01
MPA	MSE	**100%**	1.0674e-15	3.4118e-14	9.9045e-15	5.0000e-01	8.0000e-01	2.0000e-01	−1.0000e-01	2.0000e-01
	MAE	**100%**	7.2358e-08	3.7523e-07	3.2081e-07	5.0000e-01	8.0000e-01	2.0000e-01	−1.0000e-01	2.0000e-01
	MAPE	**100%**	2.5000e-01	2.5000e-01	2.5000e-01	5.0000e-01	7.9999e-01	2.0000e-01	−1.0000e-01	2.0000e-01
	MedAE	76%	3.7479e-07	6.7040e-06	2.6834e-06	5.0000e-01	8.0004e-01	2.0000e-01	−1.0000e-01	2.0000e-01
	RMSE	**100%**	3.6725e-08	1.4062e-07	1.3072e-07	5.0000e-01	8.0000e-01	2.0000e-01	−1.0000e-01	2.0000e-01
PSO	MSE	0%	3.5437e-09	4.3742e-02	2.7267e-04	4.9902e-01	3.6452e-01	1.9828e-01	−9.8164e-02	2.0025e-01
	MAE	0%	5.3031e-04	4.8119e-02	2.3822e-02	4.9823e-01	1.1330e-01	1.9820e-01	−1.0014e-01	2.0055e-01
	MAPE	0%	2.5083e-01	7.1076e-01	7.1251e-01	4.9939e-01	1.0659e-01	1.9573e-01	−9.8933e-02	2.0002e-01
	MedAE	0%	1.1231e-03	4.4399e-02	4.1492e-02	4.9636e-01	−3.5585e-01	1.9494e-01	−9.3573e-02	2.0214e-01
	RMSE	0%	2.7535e-04	3.7219e-02	1.3600e-02	4.9928e-01	4.5244e-01	1.9848e-01	−1.0034e-01	2.0024e-01
SCSO	MSE	0%	5.6284e-06	1.6141e-03	4.3886e-04	4.9854e-01	1.8109e-03	1.9831e-01	−1.0061e-01	2.0106e-01
	MAE	0%	4.8035e-03	4.5372e-02	2.1372e-02	4.9805e-01	3.0998e-03	1.9812e-01	−9.9118e-02	2.0022e-01
	MAPE	0%	2.5080e-01	3.1172e-01	2.6408e-01	4.9859e-01	−8.0075e-02	1.9801e-01	−9.9305e-02	2.0008e-01
	MedAE	0%	4.0230e-04	3.7501e-02	3.5639e-02	4.9724e-01	9.6534e-02	1.9724e-01	−1.6487e-03	2.0059e-01
	RMSE	0%	8.9900e-04	3.4641e-02	2.2373e-02	4.9850e-01	5.70571e-03	1.9906e-01	−9.9924e-03	2.0038e-01

Table 6. Statistical results of parameter identification on MCM under five objective functions.

Algorithm	J	*Acc* (%)	Best J	Mean J	Median J	$a = 2$	$b = 1$	$x_0 = 0.001$	$y_0 = 0.001$
ACGO	MSE	**84%**	0	1.5258e-07	0	2.0000e+00	1.0000e+00	1.0000e-03	1.0000e-03
	MAE	76%	0	1.1561e-04	0	2.0000e+00	1.0000e+00	1.0000e-03	1.0000e-03
	MAPE	68%	0	7.4479e-02	0	2.0000e+00	1.0000e+00	1.0000e-03	1.0000e-03
	MedAE	60%	0	4.2779e-04	0	2.0000e+00	1.0000e+00	1.0000e-03	1.0000e-03
	RMSE	82%	0	1.7571e-04	0	2.0000e+00	1.0000e+00	1.0000e-03	−1.0000e-03
CGO	MSE	**82%**	0	1.7135e-07	0	2.0000e+00	1.0000e+00	1.0000e-03	1.0000e-03
	MAE	64%	0	2.0112e-04	0	2.0000e+00	1.0000e+00	1.0000e-03	1.0000e-03
	MAPE	66%	0	6.5452e-02	0	2.0000e+00	1.0000e+00	1.0000e-03	1.0000e-03
	MedAE	68%	0	3.5203e-04	0	2.0000e+00	1.0000e+00	1.0000e-03	1.0000e-03
	RMSE	70%	0	2.9241e-04	0	2.0000e+00	1.0000e+00	1.0000e-03	1.0000e-03
DE	MSE	0%	5.7101e-09	5.8802e-07	3.7316e-07	1.9092e+00	9.0104e-01	1.5194e-03	1.8205e-01
	MAE	0%	5.2803e-05	5.3265e-04	4.1470e-04	1.9518e+00	9.5771e-01	1.3706e-03	2.0339e-01
	MAPE	0%	2.8666e-01	4.3666e-01	4.2052e-01	1.8414e+00	8.7084e-01	9.9401e-03	1.4804e+00
	MedAE	0%	9.8707e-05	1.7452e-03	9.4137e-04	1.9590e+00	9.5865e-01	1.4095e-03	2.1658e-01
	RMSE	0%	4.4338e-05	6.2592e-04	5.0151e-04	1.9334e+00	9.2156e-01	1.4108e-03	3.3352e-01
FODE	MSE	**52%**	0	3.5752e-06	4.0047e-19	2.0000e+00	1.0000e+00	1.0000e-03	1.0000e-03
	MAE	2%	0	7.2746e-04	3.3806e-06	2.0000e+00	1.0000e+00	1.0007e-03	4.0438e-02
	MAPE	14%	0	1.7017e-01	2.3330e-01	2.0000e+00	1.0000e+00	1.4753e-03	1.8917e-01
	MedAE	6%	0	8.5850e-04	1.9246e-06	2.0000e+00	1.0000e+00	1.0006e-03	1.6251e-02
	RMSE	42%	0	9.9867e-04	4.8662e-04	2.0000e+00	1.0000e+00	1.0000e-03	1.0432e-03
GWO	MSE	0%	4.9266e-13	8.1973e-06	6.7919e-09	2.0026e+00	1.0004e+00	1.0080e-03	1.4537e-01
	MAE	0%	3.4193e-06	1.6634e-03	5.0575e-04	2.0002e+00	9.9965e-01	1.0152e-03	−1.5960e-01
	MAPE	0%	1.9859e-04	1.2109e-01	6.7106e-03	2.0004e+00	9.9998e-01	1.0190e-03	9.9519e-02
	MedAE	0%	2.5396e-06	3.1372e-03	1.0090e-03	2.0000e+00	9.9989e-01	1.0081e-03	2.3641e-01
	RMSE	0%	2.2280e-06	9.1877e-04	5.0650e-05	2.0029e+00	1.0007e+00	1.0414e-03	9.2239e-02
MPA	MSE	6%	7.1932e-19	3.8740e-15	6.9749e-16	2.0000e+00	1.0000e+00	1.0000e-03	2.5606e-03
	MAE	0%	4.7892e-10	1.9247e-07	1.5587e-08	2.0000e+00	1.0000e+00	1.0001e-03	6.0857e-04
	MAPE	**8%**	1.4766e-07	8.0910e-03	7.0504e-07	2.0000e+00	1.0000e+00	1.0000e-03	−7.4021e-04
	MedAE	0%	1.3609e-09	4.5603e-07	1.0605e-07	2.0000e+00	1.0000e+00	1.0002e-03	−2.4330e-04
	RMSE	0%	8.3428e-10	5.4177e-08	4.2100e-08	2.0000e+00	1.0000e+00	1.0001e-03	1.7518e-03

Table 6. Continued.

Algorithm	J	Acc (%)	Best J	Mean J	Median J	$a=2$	$b=1$	$x_0=0.001$	$y_0=0.001$
PSO	MSE	0%	1.0674e-11	1.6040e-05	1.1672e-06	2.0057e+00	9.9563e-01	1.0190e-03	6.2376e-01
	MAE	0%	3.3393e-04	5.6279e-03	3.6309e-03	1.7433e+00	1.3067e-01	1.0594e-03	1.3970e+00
	MAPE	0%	7.0829e-02	5.4329e-01	5.0631e-01	2.0000e+00	1.0003e+00	2.1052e-03	1.5027e+00
	MedAE	0%	1.1435e-04	9.8265e-03	7.4752e-03	2.0000e+00	4.0616e-01	1.0522e-03	8.5913e-01
	RMSE	0%	2.7734e-06	3.2383e-03	1.3932e-03	2.0092e+00	9.4134e-01	8.7078e-04	7.6488e-01
SCSO	MSE	**2%**	1.7081e-13	1.1602e-07	5.1565e-10	2.0018e+00	1.0002e+00	1.0153e-03	−2.9901e-02
	MAE	0%	9.5339e-07	1.3345e-03	1.1698e-04	1.9999e+00	9.9982e-01	1.0147e-03	2.0566e-03
	MAPE	0%	5.8682e-04	1.8812e-01	1.7932e-01	2.0002e+00	9.9995e-01	1.0496e-03	3.2598e-03
	MedAE	0%	5.9431e-07	3.6201e-03	1.2784e-04	2.0000e+00	9.9995e-01	1.0249e-03	5.6878e-03
	RMSE	0%	4.2152e-07	6.8190e-04	4.2965e-05	2.0016e+00	1.0002e+00	1.0085e-03	−5.4455e-04

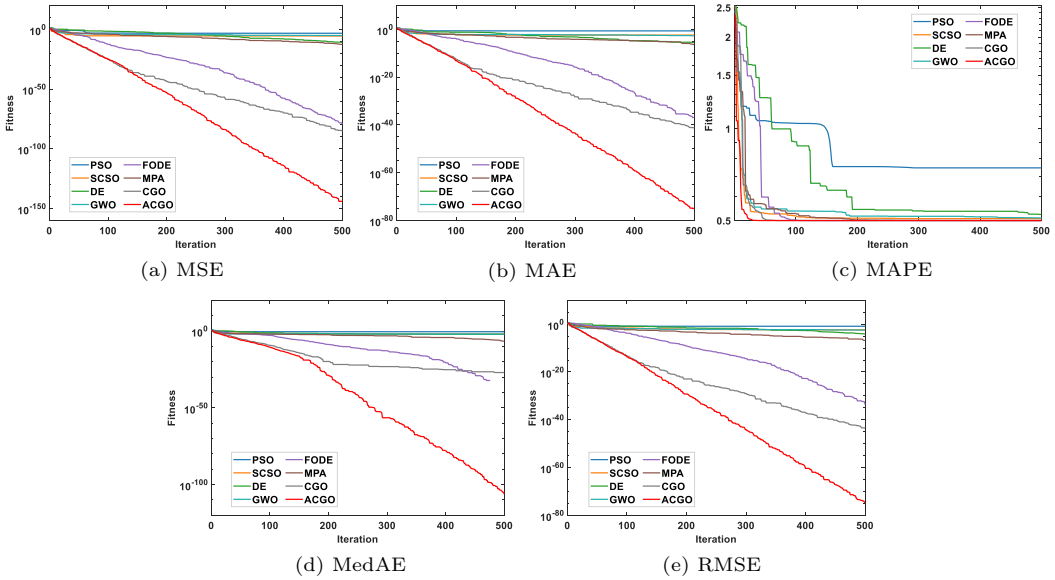
Table 7. Statistical results of parameter identification on MCNM under five objective functions.

Algorithm	J	Acc (%)	Best J	Mean J	Median J	$a=-2.5$	$b=3.5$	$k=2.15$	$x_0=0.001$	$y_0=0.5$
ACGO	MSE	34%	0	2.6909e-06	8.3437e-16	−2.5000e+00	3.5000e+00	2.1479e+00	1.0000e-03	5.0000e-01
	MAE	6%	0	9.3792e-04	4.0212e-06	−2.4608e+00	3.5000e+00	2.1472e+00	1.0000e-03	5.0000e-01
	MAPE	**74%**	0	1.4562e-02	0	−2.5000e+00	3.5000e+00	2.1500e+00	1.0000e-03	5.0000e-01
	MedAE	4%	0	1.8881e-03	5.1243e-06	−2.2383e+00	3.5000e+00	2.1492e+00	1.0000e-03	5.0000e-01
	RMSE	14%	0	7.6652e-04	1.1221e-06	−2.4042e+00	3.5000e+00	2.1389e+00	1.0000e-03	4.9928e-01
CGO	MSE	6%	2.1041e-36	2.9403e-06	3.5033e-10	−2.5001e+00	3.5000e+00	1.9041e+00	1.0000e-03	4.9928e-01
	MAE	2%	1.0842e-19	9.3943e-04	1.7129e-04	−2.4899e+00	3.5000e+00	2.1438e+00	1.0000e-03	5.0000e-01
	MAPE	**70%**	0	4.5378e-02	4.9381e-17	−2.5000e+00	3.5000e+00	2.1500e+00	1.0000e-03	5.0000e-01
	MedAE	0%	2.8351e-11	2.0534e-03	9.3577e-06	−1.2050e+00	3.5000e+00	2.1404e+00	1.0001e-03	5.0000e-01
	RMSE	8%	0	1.0870e-03	3.8122e-04	−2.1674e+00	3.5000e+00	1.8713e+00	1.0001e-03	5.0000e-01
DE	MSE	0%	1.7469e-06	1.0259e-05	1.0238e-05	−1.9860e+00	1.3375e+00	2.2610e-01	3.8749e-02	3.5759e-01
	MAE	0%	9.9987e-04	3.7262e-03	3.7195e-03	−2.1823e+00	1.1374e+00	1.2993e-01	2.4437e-02	4.3249e-01
	MAPE	0%	2.1338e-01	4.7862e-01	5.0126e-01	8.0044e-01	7.1717e-02	1.2431e+00	3.3208e-03	5.0775e-01
	MedAE	0%	5.2845e-03	7.1251e-03	7.0929e-03	−1.8925e+00	1.9837e+00	2.0323e-01	1.3284e-02	4.1454e-01
	RMSE	0%	1.4831e-03	3.1115e-03	3.1057e-03	−3.0987e+00	1.3082e+00	2.2305e-01	3.7627e-02	3.8042e-01
FODE	MSE	0%	8.8830e-19	3.0983e-06	2.3132e-06	−2.4566e+00	3.4518e+00	1.9322e+00	1.0000e-03	4.9997e-01
	MAE	0%	5.1789e-10	1.2581e-03	6.3930e-04	−1.8718e+00	3.5000e+00	1.9091e+00	1.0000e-03	4.9999e-01
	MAPE	**2%**	2.9652e-10	1.1868e-01	4.1899e-04	−2.4971e+00	3.4995e+00	2.1460e+00	1.0000e-03	5.0000e-01
	MedAE	0%	1.7742e-09	3.4670e-03	3.9354e-03	−1.2141e+00	3.0859e+00	1.3095e+00	1.0000e-03	5.0000e-01
	RMSE	**2%**	0	1.2237e-03	9.0653e-04	−4.4857e+00	3.5000e+00	1.9377e+00	1.0000e-03	5.0000e-01
GWO	MSE	0%	1.6498e-06	1.0643e-05	1.0052e-05	−2.0078e+00	9.9878e-02	−3.6235e-03	2.7382e-02	4.2431e-01
	MAE	0%	5.5880e-04	3.3771e-03	3.1658e-03	−2.0926e+00	1.7025e+00	1.2503e-02	−9.3149e-04	4.8347e-01
	MAPE	0%	4.3771e-03	2.3225e-01	1.0627e-02	−8.9554e-01	6.6034e-03	2.1349e+00	9.8696e-04	5.1063e-01
	MedAE	0%	1.1527e-03	6.9530e-03	6.9357e-03	−1.4578e+00	6.2018e-02	-3.4308e-03	3.9035e-03	5.0695e-01
	RMSE	0%	8.5477e-05	2.8324e-03	2.8945e-03	−1.6092e+00	9.6025e-01	5.7367e-02	1.7157e-02	4.7448e-01
MPA	MSE	0%	7.5271e-10	1.0029e-05	1.0218e-05	−2.6912e+00	−1.5567e-01	9.6181e-02	1.9993e-03	4.2176e-01
	MAE	0%	2.6916e-04	3.0047e-03	3.2604e-03	−1.1872e+00	1.3339e+00	2.6520e-01	4.3831e-03	4.7878e-01
	MAPE	0%	2.7432e-04	1.2750e-01	1.3310e-02	−1.8961e+00	9.4373e-01	2.1348e+00	9.9338e-04	5.0051e-01
	MedAE	0%	5.2734e-04	6.6701e-03	6.7815e-03	−1.0456e+00	1.2673e+00	1.0384e-01	1.3623e-02	4.8376e-01
	RMSE	0%	2.1126e-04	2.6945e-03	2.9542e-03	−1.7405e+00	1.6609e+00	1.5762e-01	7.2485e-04	4.8588e-01
PSO	MSE	0%	8.3081e-10	1.2148e-05	1.3493e-05	−1.4686e+00	2.6030e-01	−7.9274e-02	3.0353e-03	5.0142e-01
	MAE	0%	1.4761e-03	4.1034e-03	4.4646e-03	−1.4611e+00	−9.2123e-03	2.5662e-02	8.4310e-03	4.8936e-01
	MAPE	0%	7.4227e-03	6.5995e-01	7.8935e-01	−3.8857e-01	2.4139e-02	1.8619e-01	3.2875e-02	5.0183e-01
	MedAE	0%	5.3168e-04	7.5463e-03	7.9174e-03	−1.5025e+00	2.5456e-01	4.2840e-02	1.7124e-02	5.0018e-01
	RMSE	0%	2.9780e-04	3.1839e-03	3.3253e-03	−1.4278e+00	3.7499e-01	4.0485e-02	6.3345e-04	4.9972e-01
SCSO	MSE	0%	1.0302e-08	9.6642e-06	8.7018e-06	−3.3059e-03	5.8170e-03	1.4776e-02	1.6397e-03	4.9786e-01
	MAE	0%	1.0363e-04	3.3968e-03	3.4534e-03	−3.1224e-01	3.1462e-01	4.1922e-02	1.2898e-03	4.9973e-01
	MAPE	0%	2.5603e-03	1.9065e-01	1.0661e-02	−2.6248e-01	1.4312e-02	2.1339e+00	9.8683e-04	5.1013e-01
	MedAE	0%	2.0989e-04	7.1465e-03	6.8953e-03	−3.3011e-01	1.9859e-01	8.6875e-03	5.3759e-03	5.0171e-01
	RMSE	0%	3.5998e-04	3.0189e-03	3.0379e-03	−2.7411e-01	1.0184e+00	−2.7866e-02	8.2293e-03	4.9030e-01

The experimental results for the MSNM are listed in Table 5. It can be observed that the identification accuracy is similar to that of the MRNM, with ACGO achieving relatively high identification accuracy. Moreover, under MSE, most algorithms achieve 100% *Acc*, whereas the identification accuracy is lower under other objective functions. Consequently, MSE enables better parameter identification and improves overall performance. The convergence curves are illustrated in Fig. 6. The difference between the convergence curves of the ACGO and CGO algorithms is very small, with ACGO showing faster convergence under MSE, MAE, and MedAE.

The statistical results for the MCM are summarized in Table 6. Under MSE, ACGO and CGO achieve relatively high accuracy, which is higher than that obtained under other objective functions. The ACGO algorithm achieves 84% *Acc*, and its overall performance is better than that of the other algorithms. The convergence curves are plotted in Fig. 7. A rapid initial convergence trend is observed for both ACGO and CGO, with near-zero error levels being reached within the first 300 iterations. In the MCM experiment, ACGO and CGO perform similarly; however, overall, the identification accuracy and convergence speed of ACGO are slightly better.

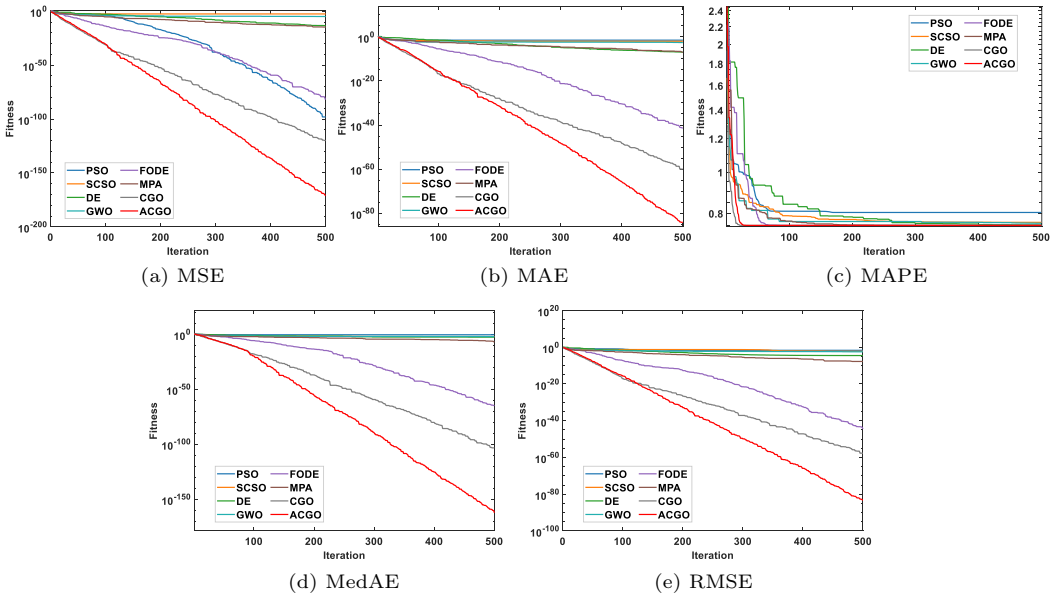
The results of parameter identification on MCNM are presented in Table 7. The findings indicate that, due to the high complexity of the system, none of the algorithms can fully and effectively achieve parameter identification for this system. Under the MAPE objective function, ACGO and CGO achieve relatively higher identification accuracies of 74% and 70%, respectively. The convergence curves are illustrated in Fig. 8. It is observed that the ACGO algorithm exhibits the fastest convergence rate, although its performance is close to that of CGO under the MAPE objective function.



(a) MSE (b) MAE (c) MAPE

(d) MedAE (e) RMSE

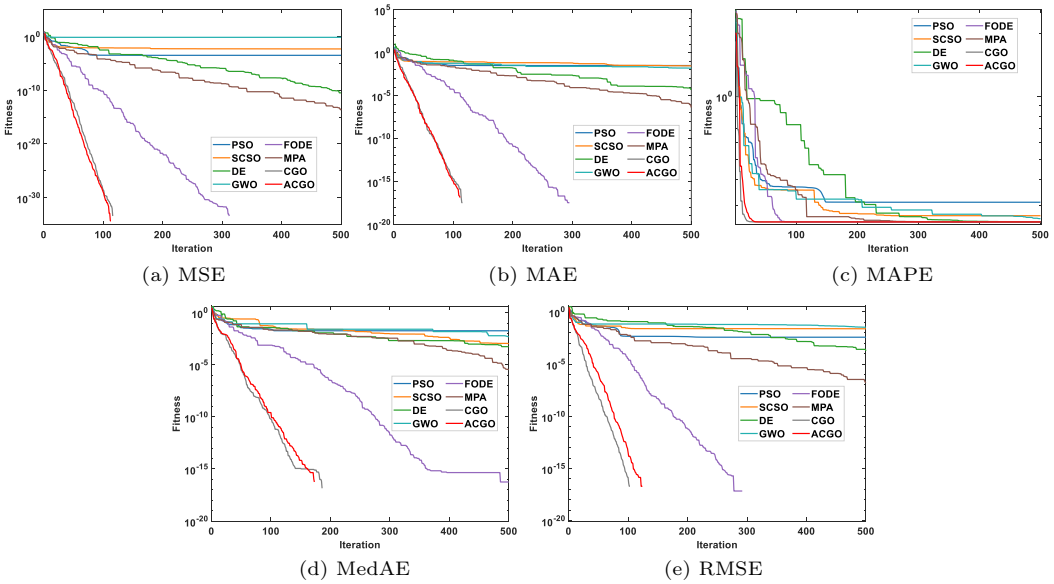
Fig. 4. Convergence curves for all intelligent optimization algorithms under MRNM.



(a) MSE (b) MAE (c) MAPE

(d) MedAE (e) RMSE

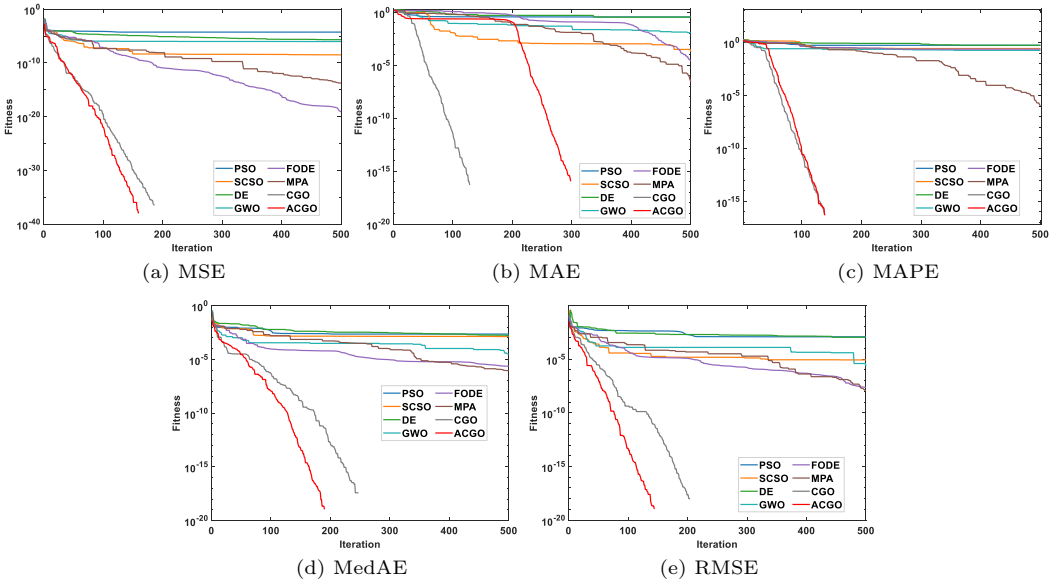
Fig. 5. Convergence curves for all intelligent optimization algorithms under MHNM.



(a) MSE (b) MAE (c) MAPE

(d) MedAE (e) RMSE

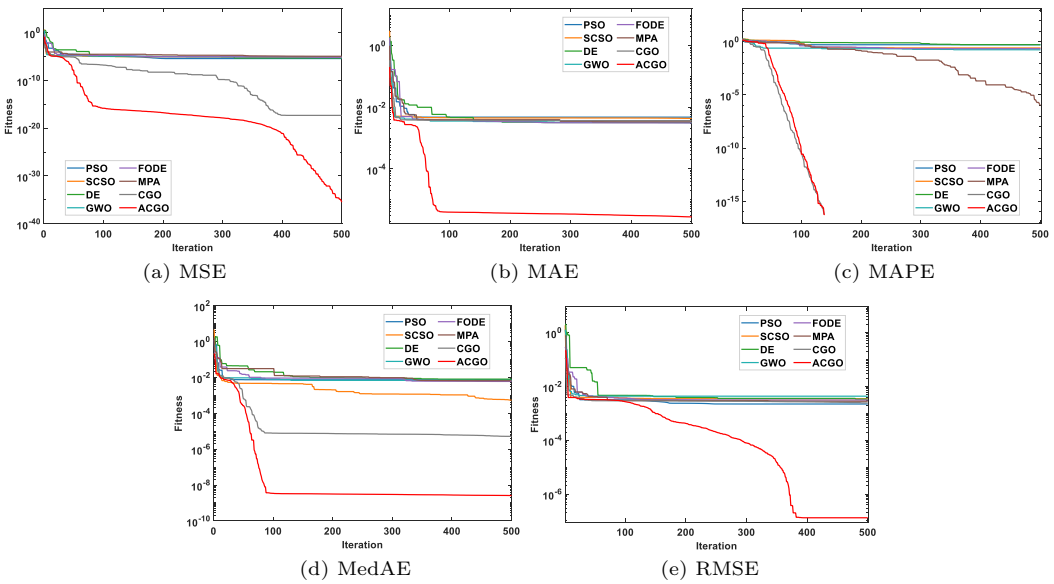
Fig. 6. Convergence curves for all intelligent optimization algorithms under MSNM.



(a) MSE (b) MAE (c) MAPE

(d) MedAE (e) RMSE

Fig. 7. Convergence curves for all intelligent optimization algorithms under MCM.



(a) MSE (b) MAE (c) MAPE

(d) MedAE (e) RMSE

Fig. 8. Convergence curves for all intelligent optimization algorithms under MCNM.

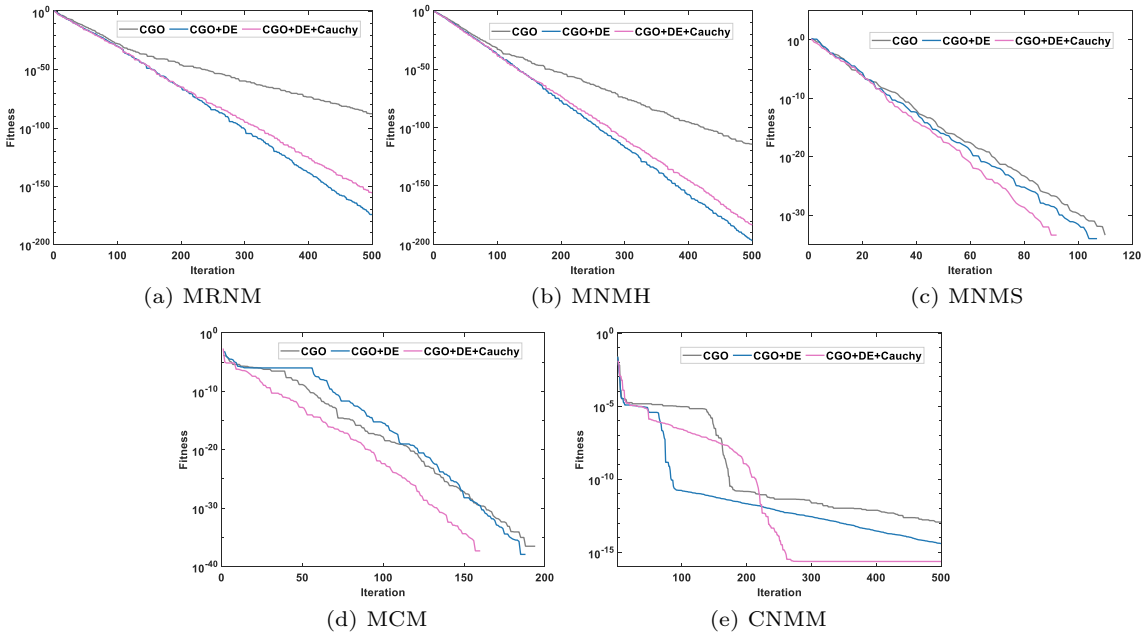
In summary, among all the algorithms, the ACGO algorithm demonstrates better performance. The MSE objective function delivers high identification accuracy for most DMNMs, indicating that MSE is more suitable for parameter identification. In contrast, other objective functions may achieve good results in some cases, but their overall performance is not as stable as that of MSE. When selecting an objective function for different optimization problems, its adaptability to the specific problem type should be considered.

4.4. Ablation study

To verify the contribution of each core improvement component in the ACGO algorithm, an ablation study was conducted. Three comparison algorithms were considered: (i) CGO: without any improved strategies; (ii) CGO+DE: introducing only the differential evolution mutation strategy; (iii) CGO+DE+Cauchy: integrating both the differential evolution mutation and Cauchy adaptive parameter strategies. The experimental results are presented in Table 8 and Fig. 9. For MRNM, MHNM, and MSNM, the improvement in J value of the CGO+DE+Cauchy algorithm is not as significant as that of the CGO+DE algorithm, but the identification accuracy has reached 100%. For MCM and MCNM, which are difficult to identify accurately, the CGO+DE+Cauchy algorithm performs better, with higher precision and faster convergence. In summary, the CGO+DE+Cauchy algorithm was selected as the final framework for the ACGO algorithm.

Table 8. Identification results of ablation study for five DMNMs.

DMNMs	Algorithms	*Acc* (%)	Best J	Mean J	Median J
MRNM	CGO	100%	3.6875e-92	3.5633e-83	1.8666e-86
	CGO+DE	100%	**3.9784e-175**	**1.3936e-167**	**1.4291e-170**
	CGO+DE+Cauchy	100%	3.6167e-159	7.7640e-146	2.0885e-152
MHNM	CGO	100%	4.8412e-122	5.7912e-113	1.5689e-117
	CGO+DE	100%	**1.6911e-203**	**2.6977e-191**	**6.0520e-197**
	CGO+DE+Cauchy	100%	8.6714e-186	2.3417e-175	5.6459e-180
MSNM	CGO	100%	0	1.9664e-33	0
	CGO+DE	100%	0	6.3171e-34	0
	CGO+DE+Cauchy	100%	0	**0**	0
MCM	CGO	82%	0	1.7135e-07	0
	CGO+DE	78%	0	2.0906e-07	0
	CGO+DE+Cauchy	**84%**	0	**1.5258e-07**	0
MCNM	CGO	6%	2.1041e-36	2.9403e-06	3.5033e-10
	CGO+DE	22%	**0**	**1.7938e-06**	8.8682e-13
	CGO+DE+Cauchy	**34%**	**0**	2.6909e-06	**8.3437e-16**



(a) MRNM (b) MNMH (c) MNMS

(d) MCM (e) CNMM

Fig. 9. Convergence curves of three algorithms under five DMNMs.

4.5. Noise interference

Noise interference is inevitable in practical engineering applications. In this subsection, additive white Gaussian noise (AWGN) is considered as the noise source. The signal-to-noise ratio (SNR) is set between 40 and 70 dB. The ACGO algorithm is adopted, with a sample size of 4 and MSE as the objective function. The obtained best values, mean values, and mean error of the identified parameters for the five DMNMs are summarized in Table 9. The mean error is defined as the mean difference between the identified parameter values and the true parameter values. The results indicate that, as the SNR increases, the mean identification error gradually decreases in the AWGN environment. Further observation shows that some system parameters of the same DMNM deviate significantly from the true values when the SNR is low and gradually converge to the true values as the SNR increases, while initial parameters such as x_0 or y_0 exhibit stronger sensitivity to noise. It is worth noting that MRNM, MHNM, and MSNM exhibit better noise robustness, while MCM and MCNM are more sensitive to noise; however, their mean error still shows a decreasing trend at high SNR levels. These results validate the effectiveness of the ACGO algorithm in noisy environments.

Table 9. Parameter identification results under noise interference.

DMNMs	Actual identified values	40 dB		50 dB		60 dB		70 dB	
		Best values	Mean values	Best values	Mean values	Best values	Mean values	Best values	Mean values
MRNM	$a=0.05$	$a=4.9530$e-02	$a=4.9338$e-02	$a=4.9939$e-02	$a=4.9849$e-02	$a=5.0019$e-02	$a=4.9945$e-02	$a=5.0012$e-02	$a=5.0007$e-02
	$b=0.05$	$b=5.0902$e-02	$b=5.0317$e-02	$b=5.0306$e-02	$b=5.0080$e-02	$b=5.0031$e-02	$b=5.0010$e-02	$b=4.9993$e-02	$b=4.9983$e-02
	$k=0.55$	$k=5.7180$e-01	$k=5.5926$e-01	$k=5.5335$e-01	$k=5.5284$e-01	$k=5.4798$e-01	$k=5.5112$e-01	$k=5.4937$e-01	$k=5.5029$e-01
	$x_0=0$	x_0=3.3856e-02	$x_0=3.4090$e-02	$x_0=1.0953$e-02	$x_0=1.1919$e-02	$x_0=2.4614$e-03	$x_0=3.6310$e-03	$x_0=1.5792$e-03	$x_0=1.1920$e-03
	$y_0=0$	$y_0=2.4009$e-03	$y_0=1.6554$e-03	$y_0=8.8316$e-04	$y_0=5.1105$e-04	$y_0=2.4985$e-05	$y_0=8.9747$e-05	$y_0=2.1730$e-04	$y_0=2.8874$e-05
	Mean error	1.1886e-02	8.1525e-03	3.1110e-03	2.8355e-03	9.1066e-04	9.3433e-04	4.8893e-04	3.0217e-04
MHNM	$a=0.25$	$a=2.4915$e-01	$a=2.4984$e-01	$a=2.5198$e-01	$a=2.5005$e-01	$a=2.5013$e-01	$a=2.5005$e-01	$a=2.5000$e-01	$a=2.5000$e-01
	$b=0.51$	$b=5.0997$e-01	$b=5.0991$e-01	$b=5.1140$e-01	$b=5.0987$e-01	$b=5.1017$e-01	$b=5.0998$e-01	$b=5.0998$e-01	$b=5.1000$e-01
	$k=-0.89$	$k=-8.6574$e-01	$k=-8.8352$e-01	$k=-8.9703$e-01	$k=-8.8871$e-01	$k=-8.8972$e-01	$k=-8.8953$e-01	$k=-8.8988$e-01	$k=-8.9013$e-01
	$x_0=0$	$x_0=1.8509$e-03	$x_0=-2.0372$e-04	$x_0=2.1695$e-03	$x_0=4.1879$e-04	$x_0=-9.6195$e-05	$x_0=1.6692$e-04	$x_0=-1.1285$e-04	$x_0=-4.9160$e-04
	$y_0=0$	$y_0=-4.8757$e-04	$y_0=5.3655$e-01	$y_0=-1.7310$e-03	$y_0=1.1151$e-04	$y_0=-1.6774$e-05	$y_0=-4.5341$e-05	$y_0=-8.5704$e-06	$y_0=1.7955$e-06
	Mean error	5.7437e-03	5.9258e-04	2.8635e-03	3.3005e-04	1.3861e-04	1.8333e-04	6.7403e-05	1.4215e-04
MSNM	$e=0.5$	$e=5.0082$e-01	$e=4.8910$e-01	$e=5.0007$e-01	$e=4.9989$e-01	$e=5.0009$e-01	$e=5.0000$e-01	$e=4.9998$e-01	$e=4.6840$e-01
	$d=0.8$	$d=9.7138$e-01	$d=7.4439$e-01	$d=8.1190$e-01	$d=7.9490$e-01	$d=8.0465$e-01	$d=7.9763$e-01	d=8.0341e-01	$d=5.7289$e-01
	$k=0.2$	$k=2.0091$e-01	$k=1.3724$e-01	$k=1.9988$e-01	$k=2.0000$e-01	$k=1.9985$e-01	$k=1.9999$e-01	$k=2.0005$e-01	$k=8.0148$e-03
	$y_0=-0.1$	$y_0=-9.8360$e-02	$y_0=-8.8202$e-02	$y_0=-9.9872$e-02	$y_0=-9.9657$e-02	$y_0=-1.0023$e-01	$y_0=-9.9924$e-02	$y_0=-9.9885$e-02	$y_0=-6.7873$e-02
	$z_0=0.2$	$z_0=2.0134$e-01	$z_0=1.9583$e-01	$z_0=2.0039$e-01	$z_0=2.0007$e-01	$z_0=2.0030$e-01	$z_0=2.0000$e-01	$z_0=1.9997$e-01	$z_0=1.8729$e-01
	Mean error	3.5218e-02	5.0423e-03	2.5231e-03	1.1879e-03	1.0847e-03	1.3939e-03	7.2355e-04	2.9023e-04
MCM	$a=2$	$a=-1.2133$e-01	$a=2.5040$e-01	$a=1.9359$e+00	$a=1.9110$e+00	$a=1.9706$e+00	$a=2.0108$e+00	$a=1.9946$e+00	$a=2.0282$e+00
	$b=1$	$b=-1.1207$e+00	$b=1.6119$e-01	$b=5.0816$e-01	$b=9.1415$e-01	$b=9.2844$e-01	$b=9.8811$e-01	$b=1.0102$e+00	$b=1.0007$e+00
	$x_0=0.001$	$x_0=1.4384$e-03	$x_0=4.0803$e-03	$x_0=4.3371$e-03	$x_0=1.9527$e-03	$x_0=1.2299$e-03	$x_0=1.2092$e-03	$x_0=1.1296$e-03	$x_0=1.0708$e-03
	$y_0=0.001$	$y_0=2.1444$e+00	$y_0=1.0693$e+00	$y_0=4.9907$e+00	$y_0=1.8972$e+00	$y_0=4.8759$e-01	$y_0=1.0551$e+00	$y_0=4.9524$e-01	$y_0=6.5268$e-01
	Mean error	1.6715e+00	9.6223e-01	1.3872e+00	3.5686e-01	1.4692e-01	8.9662e-01	1.2751e-01	6.5677e-02
MCNM	$a=-2.5$	$a=-5.0576$e+00	$a=-3.0982$e+00	$a=4.8010$e+00	$a=-2.5069$e+00	$a=-4.6007$e+00	$a=-3.1855$e+00	$a=-4.4786$e-01	$a=-2.9559$e+00
	$b=3.5$	$b=5.3809$e-01	$b=3.0722$e-02	$b=-3.9631$e+00	$b=1.8020$e-01	$b=2.0614$e+00	$b=-3.1099$e-05	$b=3.2944$e+00	$b=7.9796$e-01
	$k=2.15$	$k=7.3095$e-02	$k=-2.2965$e-02	$k=1.5486$e+00	$k=3.0946$e-01	$k=1.9679$e+00	$k=4.5228$e-01	$k=2.1418$e+00	$k=8.2861$e-01
	$x_0=0.001$	$x_0=1.8694$e+00	$x_0=8.6153$e-01	$x_0=-2.4289$e-03	$x_0=3.1412$e-01	$x_0=1.7695$e-03	$x_0=4.4910$e-01	$x_0=1.0273$e-03	$x_0=2.4725$e-01
	$y_0=0.5$	$y_0=-1.8528$e-03	$y_0=3.2260$e-01	$y_0=4.9331$e-01	$y_0=4.5433$e-01	$y_0=5.0030$e-01	$y_0=3.0974$e-01	$y_0=5.0059$e-01	$y_0=3.7262$e-01
	Mean error	1.9933e+00	1.2939e+00	3.0751e+00	1.1222e+00	7.4447e-01	1.2336e+00	4.5331e-01	9.6472e-01

5. Conclusion

In this paper, an improved chaos game optimization algorithm, named ACGO, is proposed to address the challenges of nonlinearity, multistability, and local optima in parameter identification. It incorporates the differential evolution mutation strategy and the Cauchy adaptive parameter mechanism, which effectively balance global exploration and local exploitation capabilities. Simulations are conducted on five typical DMNMs, and the results demonstrate that the ACGO algorithm outperforms other mainstream intelligent optimization algorithms, achieving higher parameter identification accuracy and faster convergence. Moreover, the effects of sample size and objective function are systematically analyzed, indicating that a sample size of $M=4$ and MSE as the objective function provide faster convergence. Finally, the ACGO algorithm exhibits strong robustness in an AWGN interference environment, further confirming its potential for practical applications.

The ACGO algorithm improves identification performance while maintaining low computational complexity, and the exploration of sample size and objective functions enhances its applicability to the control of complex nonlinear systems. Therefore, the proposed algorithm can be applied not only to the modeling of memristive neurons in neuromorphic engineering, but also extended to fields requiring precise parameter identification. Future research will focus on applying intelligent algorithms for parameter identification in practical circuit scenarios. Additionally, extending the ACGO algorithm to the parameter identification of more complex and high-dimensional DMNMs will also be a research focus.

Acknowledgments

This work was supported by the National Natural Science Foundation of China (Grant Nos. 62501516 and 62572419), the Natural Science Foundation of Hunan Province (Grant Nos. 2025JJ50391 and 2025JJ50392), and the Research Foundation of the Education Department of Hunan Province (Grant Nos. 23B0131 and 24A0124).

References

[1] Chen L Y, Muthukumar D, Natiq H, Mehrabbeik M, Lei T F and Jafari S 2025 *Chaos, Solitons Fractals* **190** 115779

[2] Strukov D B, Snider G S, Stewart D R and Williams R S 2008 *Nature* **453** 80

[3] Fossi J T, Deli V, Njitacke Z T, Mendimi J M, Kemwoue F F and Atangana J 2022 *Nonlinear Dyn.* **109** 925

[4] Ma M L, Yuan Z Y, Kalsoom U, Deng W Z and He S B 2025 *Chin. Phys. B* **34** 100502

[5] Wan Y, Zhou L Q and Han J P 2025 *Eng. Appl. Artif. Intell.* **147** 110290

[6] Guo M, Sun J H, Dou G and Iu H H C 2025 *IEEE Trans. Circuits Syst. I* **72** 5998

[7] Cao H L, Wang Y, Banerjee S, Cao Y H and Mou J 2024 *Chaos, Solitons Fractals* **179** 114466

[8] Guo Y T, Ma J, Zhang X F and Hu X K 2024 *Sci. China Technol. Sci.* **67** 1567

[9] Hong Q H, Jiang H Y, Xiao P D, Du S C and Li T 2025 *IEEE Trans. Comput.* **74** 996

[10] Xiao P D, Gu Y L, Jiang H Y, Huan Z, Du S C and Hong Q H 2025 *IEEE Trans. Comput.-Aided Des. Integr. Circuits Syst.* **44** 1234

[11] Zhang S H, Ma P, Zhang H L, Lin H R and Wang C 2024 *Nonlinear Dyn.* **113** 2667

[12] Zhang J L, Bao H, Gu J X, Chen M and Bao B C 2024 *Chaos, Solitons Fractals* **185** 115157

[13] Peng Y X, Li M L, Li Z J, Ma M L, Wang M J and He S B 2025 *Neural Netw.* **185** 107213

[14] Sun G P, Yao Z, Wang Y, Zhang X F and Xu M M 2025 *Eur. Phys. J. Spec. Top.* **234** 1724

[15] Li Y N, Lv M, Ma J and Hu X K 2024 *Nonlinear Dyn.* **112** 7541

[16] Wang X Y, Yang M, Zeng Y J, Lin Z S and Iu H H C 2025 *Cogn. Neurodyn.* **19** 97

[17] Rajagopal K, Parastesh F, Wei Z C and Sprott J C 2025 *Eur. Phys. J. Spec. Top.*

[18] Gao X H, Zhu K L and Yang F F 2025 *Chin. Phys. B* **34** 090503

[19] Snášel V, Rizk-Allah R M, Izci D and Ekinci S 2023 *Appl. Soft Comput.* **136** 110085

[20] Yin Z D, Wang L, Zhang Y J and Gao Y 2021 *Appl. Soft Comput.* **108** 107451

[21] Ebrahimi S M, Malekzadeh M, Alizadeh M and HosseinNia S H 2021 *Evol. Syst.* **12** 255

[22] Li K J, Yang X L, Li D H and Xie G J 2025 *Phys. Scr.* **100** 015291

[23] Hu Z H, Zhan J H, Li Z L, Hou X Q, Fu Z A and Yang X L 2025 *Energies* **18** 869

[24] Peng Y X, Sun S R, He S H, Zou J, Liu Y and Xia Y Z 2025 *Expert Syst. Appl.* **270** 126539

[25] Yu W, Liang H H, Chen R, Wen C L and Luo Y 2022 *Asian J. Control* **24** 2617

[26] Wang S H, Hu W, Riego I and Yu Y G 2022 *Eng. Appl. Artif. Intell.* **110** 104685

[27] Ai C Y, He S and Fan X C 2023 *IEEE Access* **11** 13724

[28] Xiong Q, She J C and Xiong J K 2023 *Symmetry* **15** 1279

[29] Huang Z K, Yang C H, Zhou X J, Gui W H and Huang T W 2023 *Appl. Intell.* **53** 18653

[30] Talatahari S and Azizi M 2021 *Artif. Intell. Rev.* **54** 917

[31] Slowik A and Kwasnicka H 2020 *Neural Comput. Appl.* **32** 12363

[32] Zhang J Q and Sanderson A C 2009 *IEEE Trans. Evol. Comput.* **13** 945

[33] Das S and Suganthan P N 2011 *IEEE Trans. Evol. Comput.* **15** 4

[34] Wang K Y, Gao S C, Zhou M C, Zhan Z H and Cheng J J 2025 *IEEE Trans. Evol. Comput.* **29** 822

[35] Mirjalili S, Mirjalili S M and Lewis A 2014 *Adv. Eng. Softw.* **69** 46

[36] Faramarzi A, Heidarinejad M, Mirjalili S and Gandomi A H 2020 *Expert Syst. Appl.* **152** 113377

[37] Wang D S, Tan D P and Liu L 2018 *Soft Computing* **22** 387

[38] Seyyedabbasi A and Kiani F 2023 *Eng. Comput.* **39** 2627

[39] Li K X, Bao H, Li H Z, Ma J, Hua Z Y and Bao B C 2022 *IEEE Trans. Ind. Inf.* **18** 1726

[40] Rong K, Bao H, Li H Z, Hua Z Y and Bao B C 2022 *Nonlinear Dyn.* **108** 4459

[41] Mou J, Ma T, Banerjee S and Zhang Y S 2024 *IEEE Trans. Circuits Syst. I* **71** 1771

[42] Li Y X, Li C B, Zhong Q, Liu S C and Lei T F 2024 *Nonlinear Dyn.* **112** 3869

[43] Xu Q, Huang L P, Wang N, Bao H, Wu H G and Chen M 2023 *Nonlinear Dyn.* **111** 20447

[44] Peng Y X, Sun K H, He S B and Alamodi O 2019 *Mod. Phys. Lett. B* **33** 1950041

[45] Li Y and Peng Y X 2023 *Fractal Fract.* **7** 811